

Field emission from molybdenum carbide

Ambrosio A. Rouse, John B. Bernhard, Edward D. Sosa, and David E. Golden

Citation: [Applied Physics Letters](#) **76**, 2583 (2000); doi: 10.1063/1.126415

View online: <http://dx.doi.org/10.1063/1.126415>

View Table of Contents: <http://scitation.aip.org/content/aip/journal/apl/76/18?ver=pdfcov>

Published by the [AIP Publishing](#)

Articles you may be interested in

[Enhancement of emission characteristics for field emitters by N-doped hydrogen-free diamond-like-carbon coating](#)

J. Vac. Sci. Technol. B **17**, 246 (1999); 10.1116/1.590507

[Field emission from ZrC and ZrC films on Mo field emitters](#)

J. Vac. Sci. Technol. B **16**, 2057 (1998); 10.1116/1.590214

[Effects of thermal annealing on emission characteristics and emitter surface properties of a Spindt-type field emission cathode](#)

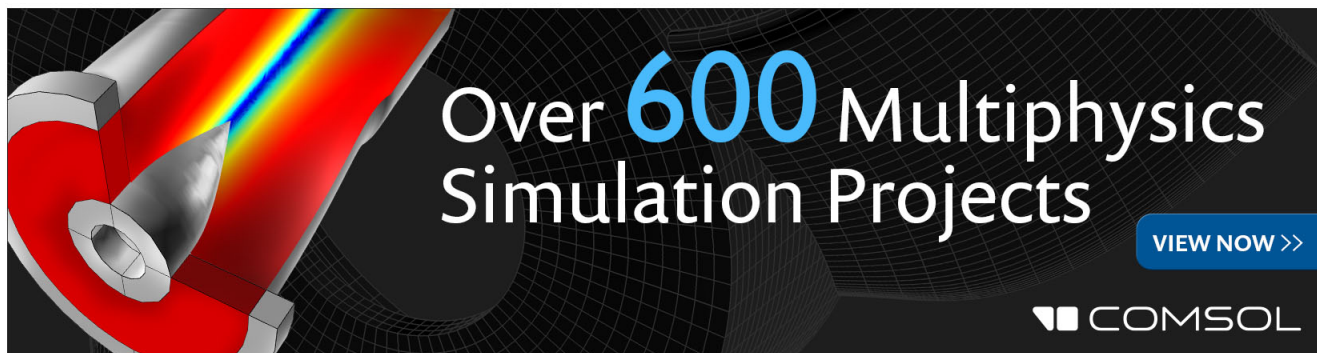
J. Vac. Sci. Technol. B **16**, 783 (1998); 10.1116/1.590218

[Surface application of molybdenum silicide onto gated poly-Si emitters for enhanced field emission performance](#)

J. Vac. Sci. Technol. B **16**, 866 (1998); 10.1116/1.589922

[Effects of thermal annealing on emission characteristics and surface properties of field emitter arrays](#)

J. Appl. Phys. **82**, 6267 (1997); 10.1063/1.366513

The advertisement features a dark background with a grid pattern. On the left, there is a 3D simulation of a mechanical part with a red and yellow color gradient. The text 'Over 600 Multiphysics Simulation Projects' is prominently displayed in the center. Below this text, there is a blue button with the text 'VIEW NOW >>'. In the bottom right corner, the COMSOL logo is visible, consisting of a small square icon followed by the word 'COMSOL'.

Field emission from molybdenum carbide

Ambrosio A. Rouse, John B. Bernhard, Edward D. Sosa, and David E. Golden^{a)}

Department of Physics and Material Science, University of North Texas, Denton, Texas 76203

(Received 23 November 1999; accepted for publication 13 March 2000)

The thermal stability and the resiliency of molybdenum carbide field-emission tips deposited at room temperature by electrophoresis have been studied. The field emission from Mo₂C films deposited on Mo tips does not change after being heated to 800 °C while exposed to 360 L of air, although MoO₂, MoO₃, and possibly MoO, are present in the films. The field-emission thresholds agree with photoelectric work functions determined from photoelectron spectroscopy measurements of similarly grown flat samples. These films are found to exist in three distinct phases as a function of temperature after formation by room-temperature electrophoresis. From room temperature to 500 °C, MoO₃ is the dominant oxide, from 500 to 775 °C, MoC₂ is the dominant oxide, and above 825 °C both oxides have virtually disappeared. © 2000 American Institute of Physics.

[S0003-6951(00)04218-2]

Cold high-brightness electron sources have been made using molybdenum field-emission arrays (FEAs) based on micron-sized field emitters deposited using the Spindt deposition process.¹ Molybdenum has been the emitter material of choice for FEAs because it has good thermal, mechanical, and electrical properties and easy to achieve high-aspect ratios.² However, when molybdenum emitters are exposed to oxygen, they easily form insulating molybdenum oxides that degrade the emission.³ In fact, when a Mo FEA was exposed to 10 L of O₂, the work function of the FEA increased by 0.3 eV and when exposed to 100 L of O₂, its work function increased by 0.6 eV. This corresponded to a decrease in emission current of 17% for 10 L exposure and 50% for 100 L at the 60 V operating voltage.³

Molybdenum carbide has a density, hardness, melting point, coefficient of thermal expansion, and conductivity similar to that of molybdenum,⁴ and could also be used to make Spindt FEAs. Molybdenum carbide has a work function of 3.8 eV,⁵ which is considerably lower than that of molybdenum with a work function of 4.6 eV,^{6,7} but it has not been investigated as a potential field emitter material.

In the present work, field emission (FE) from molybdenum carbide-coated field-emission tips has been studied in a single gated-diode configuration before and after exposure to air at 10⁻⁷ Torr and temperatures as high as 800 °C. Fowler–Nordheim FE current–voltage characteristics and simultaneous FE energy distributions (FEEDs) were obtained from tips mounted in a gated-diode configuration in the analysis chamber of a VG-ESCALAB system. In a Fowler–Nordheim plot, the natural log of the ratio of current to voltage squared (I/V^2) is plotted versus $1/V$. The slope of the resulting straight line yields the product of the work function of the surface to the 3/2 power times the “tip-shape parameter.” Since the work function may be directly measured with a FEED, a straight-line current–voltage characteristic insures that the tip-shape function did not change during the FEED measurement.

Molybdenum carbide-coated tip FE thresholds have been

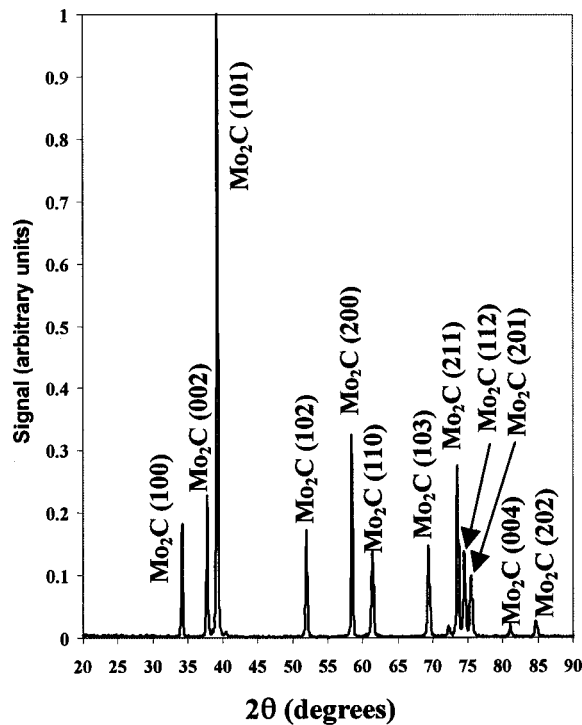
determined from FE energy distribution measurements and compared to ultraviolet photoelectron spectroscopy (UPS) measurements using similarly coated flat samples. These samples also have been studied using x-ray photoelectron spectroscopy (XPS) and x-ray diffraction (XRD) as a function of annealing.

FE tips were fabricated from 0.02-in.-thick molybdenum wire that was electrochemically etched in a 2 mol % KOH solution using a +10 V bias voltage on the wire and then rinsed in distilled water. Molybdenum carbide powder (99.5%) of 3–4 μm average size was mixed in an aqueous solution of 10% ethanol and used to deposit molybdenum carbide via electrophoresis⁸ on the tips and molybdenum foils at room temperature by applying a +240 V bias to the sample for 10 min.⁹

Flat samples were processed in a chamber attached to a VG ESCALAB II system over a temperature range from 26 to 900 °C in 1 h intervals at an average base pressure of 1 × 10⁻⁷ T of air. Additional samples were annealed at 412, 525, and 800 °C in 1 h intervals at an average base pressure of 10⁻⁷ T of air. All samples were characterized with XPS before and after each annealing stage and with scanning electron microscope (SEM) micrographs taken with a JEOL JMS-T300 before processing and analysis, and after analysis. Low-energy (4.49, 5.06, and 5.64 eV) UPS data with a Xe UV source and 2 nm bandpass monochromator also were obtained. UPS and XPS data were analyzed with the PEAKFIT program using Gaussian profiles.¹⁰ XRD was obtained with a Siemens D500 diffractometer using Cu Kα₁ radiation.

The XRD result for Mo₂C deposited on a flat Mo sheet is given in Fig. 1 and corresponds to hexagonal Mo₂C.¹¹ The three major Mo₂C peaks found in Mo₂C powder are clearly seen. In addition, the intense Mo (200) peak drops by a factor of 2.5 after Mo₂C deposition, indicating good Mo₂C coverage. A slight shift of the diffraction lines toward lower 2θ angles between the deposited samples and the Mo₂C powder was seen, indicating lattice expansion. This is likely due to oxygen substitution for carbon, as previously reported.¹² This stress was relieved with increasing annealing temperature. Finally, the MoO₃ (002), (200), and (101) planes are

^{a)}Electronic mail: golden@unt.edu

FIG. 1. XRD for a Mo₂C film.

present in the XRD results, although this cannot be seen in Fig. 1. The flat samples were annealed in the processing chamber over a temperature range from 26 to 900 °C in 1 h intervals at an average base pressure of 1×10^{-7} T to investigate the surface constituents of the Mo₂C films. These samples were characterized with XPS before and after each annealing stage and with SEM micrographs before and after processing. The XPS spectra contained the Mo 3*d* and Mo 3*p* doublets, and the C 1*s* and O 1*s* peaks. The Mo 3*d* doublet was used to indicate the presence of MoO₃ and MoO₂ by stoichiometry. Table I has the peak height ratios of the O 1*s*/C 1*s*, O 1*s*/Mo 3*d*_{5/2}, C 1*s*/Mo 3*d*_{5/2}, and the Mo 3*d*_{5/2}/Mo 3*d*_{3/2} peaks during annealing at different temperatures. As can be seen by reference to the O 1*s*/Mo 3*d*_{5/2} and O 1*s*/C 1*s* ratios, the O content initially increases and then decreases with increasing temperature. However, both the C 1*s*/Mo 3*d*_{5/2} and Mo 3*d*_{5/2}/Mo 3*d*_{3/2} ratios show three distinct temperature regimes. The transition temperatures between the first and second (~ 525 °C) and between the second and third (~ 800 °C) regimes agree with the reported desorption temperatures for MoO₂ (Ref. 13) and MoO₃.¹⁴ Examination of the C1*s* structure below 775 °C shows several peaks attributed to various states of adsorbed CO on

TABLE I. Peak ratios with annealing temperature.

<i>T</i> (°C)	C/Mo _{5/2}	O/Mo _{5/2}	O/C	Mo _{5/2} /Mo _{3/2}
26	0.5	1.5	3.1	1.2
500	0.4	1.5	3.7	1.1
650	0.7	1.9	2.7	0.6
725	0.6	1.5	2.6	0.8
775	0.7	1.1	1.7	0.7
825	0.2	0.3	1.1	1.4
875	0.2	0.1	0.6	1.5
900	0.2	0.1	0.3	1.5

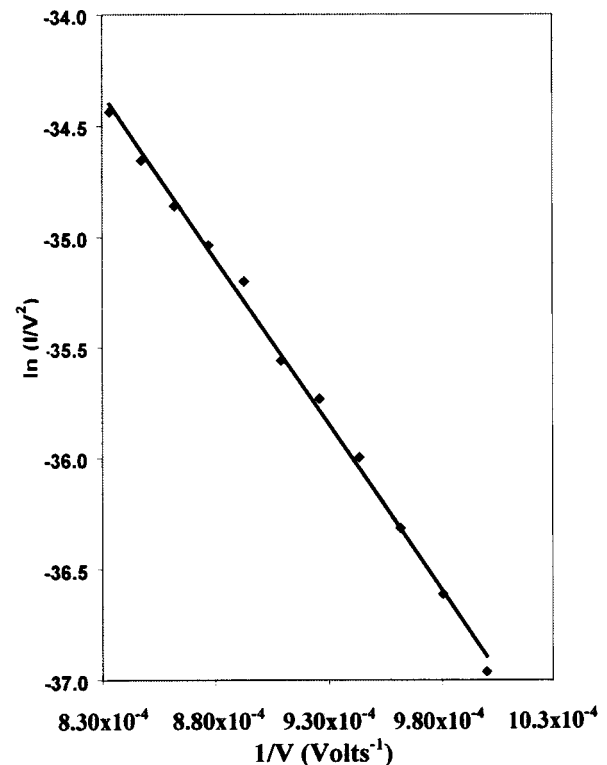
TABLE II. Mo *d*_{5/2}/Mo *d*_{3/2} ratio with annealing time.

Time (h)	Temperature (°C)		
	412	525	800
1	1.5	0.5	1.3
2	1.3	0.5	1.5
3	1.4	0.5	1.5
Average	1.4	0.5	1.4

Mo.^{15,16} There are no peaks due to adsorbed CO above 775 °C.

In the first temperature regime, CO, MoO, MoO₂, MoO₃, and Mo₂C are present, with MoO₃ the dominant molybdenum oxide. In the second phase, CO, MoO₂, MoO₃, and Mo₂C are present, with MoO₂ the dominant oxide and in the last phase, MoO₂, MoO₃ are only present in trace amounts. To further understand how the transitions between the regions where MoO₃, MoO₂, and Mo₂C dominate depend on time and temperature, the Mo 3*d*_{5/2}/Mo 3*d*_{3/2} ratio was studied as a function of time in the three regions. As may be seen in Table II, this ratio did not change over a 3 h interval, indicating that the transitions are temperature dependent and not time dependent. The sample annealed at 412 °C for 3 h contained Mo⁺⁶, indicating MoO₃ as the dominant oxide at that temperature. The sample annealed at 525 °C for 3 h showed Mo⁺⁴, indicating MoO₂ as the dominant oxide at that temperature. The sample annealed at 800 °C for 3 h, showed Mo₂C was dominant over both oxides at that temperature.

Figure 2 shows a Fowler–Nordheim plot and Fig. 3 shows FEED spectra for the same nonannealed tip. During the measurements, the tip bias was -89.99 V with an anode voltage that ranged from 1000 to 1200 V in 50 mV steps and

FIG. 2. Fowler–Nordheim plot for a nonannealed Mo₂C tip.

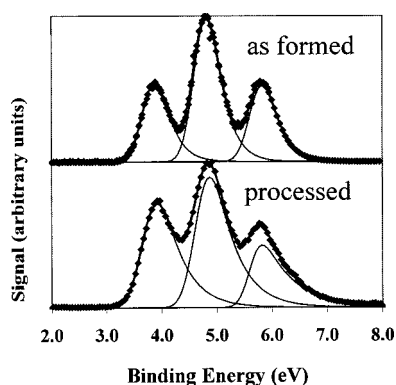


FIG. 3. FEED for a nonannealed compared to an annealed tip.

an analyzer resolution of 0.1 eV. The FEED in Fig. 3 is the average of normalized energy distributions obtained at each voltage on the I - V plot. Three well-defined peaks are seen that have been fitted with exponentially modified Gaussian functions using the PEAKFIT program.¹⁰ The peaks have inflection points at 3.7, 4.7, and 5.7 eV, respectively. FE thresholds are given by the energies at inflection points of the FEED contributions.^{7,9} The first two energies are in good agreement with the accepted values for the work functions of Mo_2C (Ref. 5) and Mo,^{6,7} respectively. The 5.7 eV threshold is attributed to a deeper state of Mo. Figure 3 also shows a FEED for the same Mo_2C tip heated to 800 °C and exposed to 360 L of air at 10^{-7} Torr for 1 h in the processing chamber attached to the VG-ESCALAB system. These data are plotted on the same scale as used for the nonannealed data and have been fitted with three peaks that have points of inflection at 3.7, 4.7, and 5.6 eV, respectively. Thus, the work function of Mo_2C does not vary with an exposure of 360 L of air. This is much different than the 6.4% and 12.8% increases in work function found for Mo with 10 and 100 L exposures to O_2 .³

Low-energy UPS spectra were obtained using 5.64, 5.06, and 4.49 eV incident photons. The data and best fits to the data using the PEAKFIT program¹⁰ with Gaussian functions are shown plotted in Fig. 4 as a function of binding energy (energy difference between photon energy and the ejected electron kinetic energy) at each photon energy used. The energy scale measures the energy difference between the vacuum level and populated levels below the vacuum level. Peaks at averaged energies of 2.9, 3.8, and 4.3 eV are obtained at all three photon energies. A peak at 1.7 eV is obtained with 4.49 eV photons, a peak at 4.7 eV with 5.06 and 5.64 eV photons, and a peak at 5.2 eV with 5.64 eV photons. The 3.8 eV result can be attributed to Mo_2C (Ref. 5) and the 4.7 eV result can be attributed to Mo,^{6,7} while the peaks at 1.7, 2.9, and 4.3 eV are attributed to Mo oxides. The 2.9 eV peak could be due to MoO that has a reported transition at 2.6 eV in its photoelectron spectra.¹⁷ The peak at 5.2 eV is likely due to the deeper state of Mo seen at 5.6 eV in the FEED discussed above.

Molybdenum carbide is found to be an excellent material for field emitter tips. Molybdenum carbide films are easy to deposit and are resilient to exposure up to 360 L of air. They

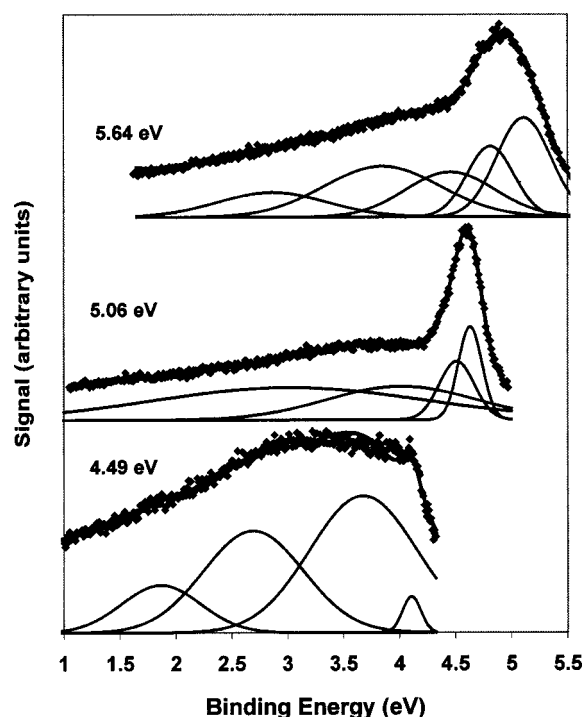


FIG. 4. UPS for 4.49, 5.06, and 5.64 eV photons.

have a 17% lower work function than Mo and make extremely good field emitter surfaces, even with significant oxygen content.

The authors would like to thank Professor Teresa Golden of the Chemistry Department at the University of North Texas for allowing them to do the XRD studies in her laboratory. This work is supported in part by the NSF through Grant No. DMR-9705187.

¹C. A. Spindt, J. Appl. Phys. **39**, 3504 (1968).

²M. S. Mousa, Vacuum **45**, 241 (1993).

³B. R. Chalamala, R. M. Wallace, and B. E. Gnade, J. Vac. Sci. Technol. B **16**, 2859 (1998).

⁴Handbook of Chemistry and Physics, 77th ed., edited by D. R. Lide and H. P. R. Fredericks (CRC Press, 1996).

⁵V. S. Fomenko, in Handbook of Thermionic Properties, edited by G. V. Samsonov (Plenum, New York, 1966).

⁶D. E. Eastman, Phys. Rev. B **2**, 1 (1970).

⁷J. M. Bernhard, A. A. Rouse, E. D. Sosa, B. E. Gnade, and D. E. Golden, Rev. Sci. Instrum. **70**, 3299 (1999).

⁸A. T. Andrews, Electrophoresis, Theory, Techniques, and Biochemical and Clinical Applications (Clarendon, Oxford, 1986).

⁹This process has been used to deposit diamond on Mo substrates; see A. A. Rouse, J. B. Bernhard, E. D. Sosa, and D. E. Golden, Appl. Phys. Lett. **75**, 3417 (1999).

¹⁰PEAKFIT, SSPS, Inc., 444 North Michigan Avenue, Chicago, IL 60611.

¹¹International Centre for Diffraction Data, 12 Campus Blvd., Newton Square, PA 19073-3273.

¹²J. W. Rabalais and R. J. Colton, Chem. Phys. Lett. **29**, 131 (1974).

¹³W. Listowski, A. H. J. van den Berg, I. J. Hanekamp, and A. van Silfhout, Surf. Interface Anal. **19**, 93 (1992).

¹⁴D. Wang, M. H. Lunsford, and M. P. Rosynek, J. Catal. **169**, 347 (1997).

¹⁵C. Zhang, M. A. Van Hove, and G. A. Somorjai, Surf. Sci. **149**, 326 (1985).

¹⁶E. V. Rut'kov, A. Ya. Tontegode, M. M. Usufov, and N. R. Gall, Sov. Phys. Tech. Phys. **37**, 1038 (1982).

¹⁷R. F. Gunion, S. J. Dixon-Warren, and W. C. Lineberger, J. Chem. Phys. **104**, 1765 (1996).